THERMAL-HYDRAULIC PERFORMANCE OF TiO_2-WATER NANOFLUIDS IN AN OFFSET STRIP FIN HEAT EXCHANGER

by

Emre Askin ELIBOL [*] ***and Oguz TURGUT***

Department of Mechanical Engineering, Engineering Faculty, Gazi University, Ankara, Turkey

Original scientific paper
https://doi.org/10.2298/TSCI201019063E

The flow and heat transfer characteristics of the TiO_2-water nanofluid assuming as a single-phase in the rectangular offset strip fin structure for different Reynolds number (500-1000) and TiO_2 nanoparticle volume concentration values (0-4%) were investigated numerically under 3-D, steady-state, and laminar flow conditions. Simulations were also performed for 1% and 4% nanoparticle volume concentrations of Al_2O_3-water nanofluid, and the results were compared with those of TiO_2-water nanofluid. Results show that when the TiO_2-water nanofluid is used, the heat transfer rate, heat transfer coefficient, and Nusselt number increase with increasing both Reynolds number and nanoparticle volume concentration, and parallel to these, both pressure loss, and pumping power increase. Considering the values of the performance evaluation criteria number, it is clear that the use of TiO_2-water nanofluid in offset strip fin structure at all Reynolds numbers examined between 1-4% volume concentration values is quite advantageous. It is observed that TiO_2-water nanofluid is much superior to Al_2O_3-water considering the performance evaluation criteria number. When the Reynolds number is 1000 and the volume concentration value of the TiO_2 nanoparticle is 4%, the performance evaluation criteria number value is found to be 1.19, that is, there is a 19% increase compared to water. It is considered that the results of this study can be used as important data on the design of automobile radiators, air-conditioning, and defense.

Key words: *plate-fin heat exchanger, offset strip fin, nanofluid, heat transfer, pressure drop*

Introduction

Compact heat exchangers are frequently preferred in aerospace applications, automobile, and cryogenic industries due to their compact structure for desired thermal performance, resulting in weight, reduced space, support structure, energy requirement, footprint and cost [1]. The plate-fin heat exchangers, a type of compact heat exchanger, have a wide variety of applications. Several fin structures have been developed by shaping the fin geometries to be used in these applications: wavy, perforated, plain, offset-strip, louvered*, etc.* Surfaces formed by these fins, which are enhanced or augmented extended surfaces, have been rather effective in increasing both the heat transfer coefficient and the surface area density [2-4]. Amongst these fins, offset strip fins characterized by substantial heat transfer enhancement, large heat transfer area, lightweight per unit volume, higher degree of surface compactness and remarkable structural endurance are quite suited as heat transfer fins in motor vehicle industry [5], especially in engine cooler of heavy vehicles that require high cooling performance. The engine cooling

[*] Corresponding author, e-mail: emreaskinelibol@gmail.com

system is used to cool the engine blocks, which can guarantee low emissions and compactness as well as ensure the safe operation and life of the engine.

The heat transfer enhancement in offset strip fins stems from enlarging surface area and the restarting of the thermal boundary-layers at the end of each fin module which causes a decrease in the average boundary-layer thickness in the line compared to uninterrupted fin geometries and induces higher heat transfer coefficient as the fluid-flows through the fin line. Regeneration of thermal boundary-layer in each flow channel, the periodic interruption on the boundary-layers and the oscillating velocity occur in the entire fin passages. Their progressive surfaces interrupt temperature boundary-layers and stream lines along flow orientation and induce vortexes and entrance effects as well as preventing fully developed flow [6]. Thermal entry length effect results in increasing heat transfer characteristics [7]. However, along with the augmentation of the heat transfer coefficient, the interrupted arrays and successive boundary-layer restarting's trigger a large pressure drop arising from the increased drag and skin friction contribution due to the finite length of the each fin modules as well. Because of this contrary phenomenon, in the evaluation of the overall performance of an offset strip fins, pressure drop and related pumping power together with the enhanced heat transfer findings should be considered [8].

In the past few decades, many researchers [5, 9-17] experimentally studied the flow and heat transfer characteristics of offset strip fins. Correlations for Colburn *j*-factor and Fanning friction factor were developed in some of these [5, 9, 10, 13, 14, 16]. Some of them investigated the effect of geometric parameters such as fin space, fin height, fin thickness, and fin length by using existing correlations [12, 17]. In recent years, with the development of CFD software, numerical studies [1, 18-30] have been carried out to investigate the thermal-hydraulic behaviors of different working fluids such as air, water, and cryogenic fluid in the offset strip fins. In addition, in some of these studies, geometric parameters have been tried to be optimized in order to benefit from the maximum heat transfer performance of offset strip fins. However, as is known, the production of such fins is made with molds and, therefore, it is not possible to manufacture according to every desired geometric parameter. Changing the geometric parameters of the fins has now reached its limits in consequence. Besides, the thermal conductivity of conventional coolants such as water-ethylene glycol mixture and oil, which are currently used in plate-fin heat exchangers with offset strip fins in engine cooling systems, are very low. For the aforementioned reason, it is necessary to use a fluid with a higher thermal conductivity in terms of heat transfer in this type of heat exchangers instead of conventional coolants.

With the development of production techniques, metallic and non-metallic particles in nanometer size have added into base fluid in order to increase heat transfer. It is thought that this new coolant class, called nanofluid, will replace conventional coolants in engineering applications in the near future [31]. Due to the superior thermal properties of these nanofluids compared to conventional coolants, they have the potential to be used in a wide variety of applications where the heat transfer occurs [32]. In particular, nanofluids have a great ability to increase the cooling performance of the cooling systems in automobile and heavy vehicle engines as well as reducing the dimensions and, therefore, weight of these systems [33-37]. Among the wide variety of nanofluids, titanium dioxide TiO_2, in particular, is very prominent with regards to its stabile and non-toxic structure and preferred by many researchers in nanofluid investigations.

Khoshvaght-Aliabadi *et al.* [16] carried out an experimental and comparative study on the performance of different plate-fin channels including offset strip fins by using the copper

deionized-water nanofluids with different volume concentrations. They concluded that the average heat transfer coefficient enhances with increasing two parameters: volumetric flow rate and volume concentration of nanoparticles. Additionally, they found that the use of nanofluid in all fin structures is quite advantageous at the lower flow rates and high nanoparticle volume concentrations. Zhao *et al*. [27] numerically investigated the flow and heat transfer characteristics of Al_2O_3-water nanofluids in an offset strip fins with the assumptions of single-phase, laminar flow and 3-D. Their numerical results show that both heat transfer and pressure loss of offset strip fins are improved considerably with the increase in Reynolds number and nanoparticle volume concentration.

Literature review has indicated that there is a lack of studies investigating the flow and heat transfer in the rectangular offset strip fin structure using TiO_2-water nanofluid, which is quite promising compared to other nanofluids. Therefore, in this study, the thermal-hydraulic performance of TiO_2-water nanofluid in rectangular offset strip fin structure was investigated numerically using single phase model under laminar flow condition for 3-D conjugate heat transfer. Flow and heat transfer characteristics for different Reynolds numbers (500-1000) and TiO_2 nanoparticle volume concentration values (0-4%) were investigated in detail calculating heat transfer rate, heat transfer coefficient, Nusselt number, pressure loss, and pumping power values. In addition, unlike other studies investigating nanofluid-flow in offset strip fin structure, performance evaluation criteria (PEC) numbers were also calculated in order to see whether the use of TiO_2-water nanofluid instead of water was effective.

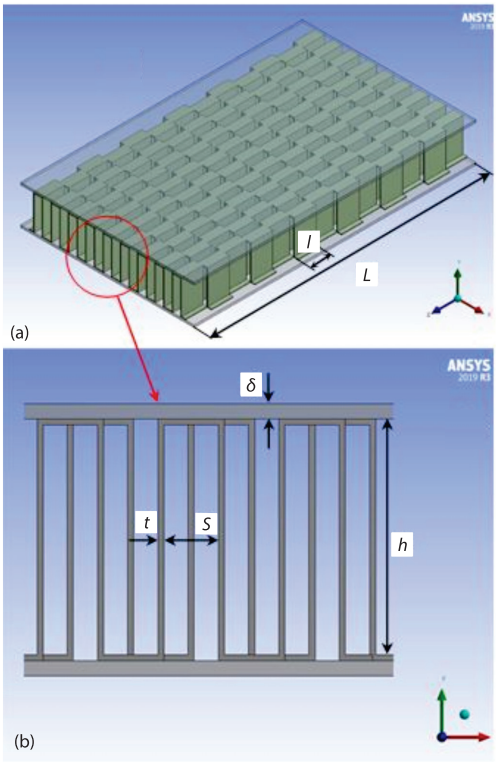

Figure 1. (a) A part of the plate-fin heat exchangers consisting of rectangular offset strip fins and (b) geometric parameters of the rectangular offset strip fins

Mathematical model

Physical model and computational domain

The geometrical parameters of rectangular offset strip fins are defined in figs. 1(a) and 1(b). A part of the plate-fin heat exchangers consisting of rectangular offset strip fins is shown in fig. 1(a). In order to better distinguish geometric parameters, some of this part is enlarged and shown in fig. 1(b). The computational domain shown in fig. 2 contains the top plate, bottom plate, offset strip fins, and working fluid volume. According to several literature studies, it is observed that the flow in rectangular offset strip fins becomes a fully developed flow after 4-5 fin modules each of l in length [19, 23]. Also, considering the periodic characteristic of the offset strip fins, channel geometry described in fig. 2 is chosen as the computational domain to shorten computational time without compromising precision of the results. Based on all these data, the present numerical study is carried out by creating the computational domain of 13 fin modules and providing fully developed flow conditions. The

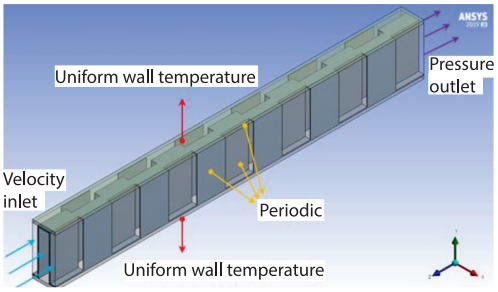

Figure 2. Computational domain with the boundary conditions

quantitative values of the geometrical parameters of the computational domain are shown in fig. 1. Channel length, L, top-bottom plate thickness, δ, fin length, l, fin thickness, t, fin space, s, and fin height, h, are 65, 0.5, 5, 0.2, 1.8, and 7.8 mm, respectively. It is seen that copper, brass, and aluminum materials are used for solid parts in industrial applications such as vehicle radiators [38]. Therefore, all solid parts defined in the computational domain are selected as copper.

Governing equations

In numerical studies using nanofluids as fluid, there are two different approaches, single-phase and two-phase [39-42]. As the manufacturing methods are developed, nanoparticles are produced in smaller sizes. Due to rather small size of nanoparticles, several researchers stated that when the nanoparticle volume concentration is very low, nanofluids act as a single-phase fluid [43, 44]. Therefore, in the present numerical study, a model with a simpler application and a shorter calculation period is preferred in the patterning of the nanofluid that is percolated through the rectangular offset strip fins. The following assumptions are considered in the solution of the flow and heat transfer phenomenon:

– the flow regime is laminar,
– the flow is a steady-state and 3-D,
– nanofluids are considered as an incompressible, single-phase and Newtonian fluid,
– nanoparticles and base fluid are in thermal equilibrium,
– nanoparticles are uniform in terms of size and shape,
– natural-convection and thermal radiation are neglected, and
– the properties of working fluids -except the thermal conductivity of Al_2O_3-water nanofluid- are constant.

With aforementioned assumptions, the laminar flow and heat transfer problem of the nanofluid in the offset strip fins is solved by the continuity, momentum and energy equations, respectively:

$$(\nabla V) = 0 \tag{1}$$

$$\rho_{\mathrm{nf}} (\nabla V) V = -\nabla P + \mu_{\mathrm{nf}} \nabla^2 V \tag{2}$$

$$\rho_{\mathrm{nf}} c_{p,\mathrm{nf}} (\nabla V) T = k_{\mathrm{nf}} \nabla^2 T \tag{3}$$

The eqs. (1)-(3) are solved using appropriate boundary conditions shown in fig. 2. At the inlet section, velocity inlet boundary condition of ANSYS FLUENT 2019 R3 is employed. Fluid enters the channel at a temperature of 300 K. Pressure outlet boundary condition is specified to the outlet, periodicity is applied on the right and left surfaces of the domain, a constant wall temperature (320 K) boundary condition is defined on the bottom and top surfaces of the plates. No-slip boundary condition is used for the walls.

Thermophysical properties of TiO_2-water and Al_2O_3-water nanofluids

The thermophysical properties of the nanofluid in the single-phase model are determined in order to carry out the numerical solution. The parameters such as nanoparticle and

base fluid type, nanoparticle volume concentration, nanoparticle size, and temperature significantly affect the thermophysical properties of nanofluids [45]. Therefore, the thermophysical properties of Al_2O_3-water, used in the validation study, and TiO_2-water nanofluids, used in the original study, should first be determined. The density, ρ_{nf}, and specific heat $c_{p,nf}$ of TiO_2-water and Al_2O_3-water nanofluids can be calculated accurately, respectively [46]:

$$\rho_{nf} = \varphi_p \rho_p + \left(1-\varphi_p\right)\rho_{bf} \tag{4}$$

$$c_{p,nf} = \frac{\left[\varphi_p \rho_p c_{p,p} + \left(1-\varphi_p\right)\rho_{bf} c_{p,bf}\right]}{\rho_{nf}} \tag{5}$$

Many studies emphasized that the Brownian motion of nanoparticles should be debated in the thermal conductivity calculation of nanofluid. Thus, in the validation study, the term $k_{Brownian}$ in eq. (6) is also taken into account while calculating the thermal conductivity of Al_2O_3-water nanofluids [47]:

$$k_{nf} = k_{static} + k_{Brownian} \tag{6}$$

where k_{static} can be calculated using Maxwell model [48]:

$$k_{static} = k_{bf}\left\{\frac{\left[\left(k_p + 2k_{bf}\right) - 2\varphi_p\left(k_{bf} - k_p\right)\right]}{\left[\left(k_p + 2k_{bf}\right) + \varphi_p\left(k_{bf} - k_p\right)\right]}\right\} \tag{7}$$

Based on [44], the term $k_{Brownian}$ contributed by the Brownian motion of Al_2O_3 nanoparticle can be determined:

$$k_{Brownian} = 5\cdot 10^4 \beta \varphi_p \rho_{bf} c_{p,bf}\sqrt{\frac{\kappa T}{\rho_p d_p}} f\left(T,\varphi_p\right) \tag{8}$$

$$f\left(T,\varphi_p\right) = \left(2.8217\cdot 10^{-2}\varphi_p + 3.917\cdot 10^{-3}\right)\left(\frac{T}{T_0}\right) + \left(-3.0669\cdot 10^{-2}\varphi_p - 3.91123\cdot 10^{-3}\right) \tag{9}$$

where $\kappa = 1.3807\cdot 10^{-23}$ J/K is the Boltzmann constant, $T_0 = 273$ K – the reference temperature, β value of Al_2O_3 nanoparticle is $8.4407(100\varphi_p)^{-1.07304}$ for $1\% \le \varphi_p \le 10\%$ and 298 K $\le T \le$ 363 K [44].

In the original study, while calculating the thermal conductivity of TiO_2-water nanofluid, temperature dependency is not taken into account. Although the temperature dependent thermal conductivity correlation for TiO_2-water nanofluid has been developed in the literature [49], this correlation is not suitable for the original numerical study, since this correlation is valid in the range of 15-35 °C. Therefore, eq. (7) is used to calculate the thermal conductivity of TiO_2-water nanofluid.

The following equations shown below can be used for the viscosity μ_{nf} of TiO_2-water and Al_2O_3-water nanofluids [50]:

$$\mu_{nf} = \frac{\mu_{bf}}{1 - 34.87\left(\frac{d_p}{d_{bf}}\right)^{-0.3}\varphi_p^{1.03}} \tag{10}$$

$$d_{bf} = \left(\frac{6M}{N\pi\rho_{bf0}}\right)^{1/3} \tag{11}$$

where M is the molecular weight of base fluid, $N = 6.022 \cdot 10^{23}$ 1/mol – the Avogadro number, and $\rho_{bf,0}$ – the density of base fluid calculated at 293 K. In addition, the basic thermophysical properties of water, the TiO_2 nanoparticle, and Al_2O_3 nanoparticle are presented in tab. 1. Present study is carried out for the nanoparticle volume concentration between 0% and 4% due to the corrosion, stability, sedimentation, pressure drop problems, and effective increase in heat transfer [45, 51-54].

Table 1. Thermophysical properties of water, Al_2O_3 and TiO_2 nanoparticles

Thermophysical properties	Water	Al_2O_3	TiO_2
Density, ρ [kgm^{-3}]	996.5	3600	4260
Specific heat, c_p [Jkg^{-}1K^{-1}]	4181	765	6890
Thermal conductivity, k [Wm^{-1}K^{-1}]	0.6103	36	11.7
Viscosity, μ [Pas]	$1003 \cdot 10^{-6}$	–	–
Diameter, d_p [nm]	–	30	30

Correlations for heat transfer and flow characteristics of the offset strip fins

While evaluating the results of numerical analysis, the heat transfer rate, $\dot{Q}$, average heat transfer coefficient, h, average Nusselt number, Nu, Reynolds number, Re, Colburn j-factor, j, Fanning friction factor, f, and pumping power, PP, can be determined, respectively [55]:

$$\dot{Q} = \dot{m} c_p \left(T_{out} - T_{in}\right) \tag{12}$$

$$h = \frac{\dot{Q}}{A_t \Delta T_{LMTD}} \tag{13}$$

$$\mathrm{Nu} = \frac{hD_h}{k} \tag{14}$$

$$\mathrm{Re} = \frac{\rho u D_h}{\mu} \tag{15}$$

$$j = \frac{\mathrm{Nu}}{\mathrm{Re}\,\mathrm{Pr}^{1/3}} \tag{16}$$

$$f = \frac{\rho D_h \Delta P}{2LG^2} \tag{17}$$

$$PP = \Delta P \dot{V} \tag{18}$$

where A_t [m^2] is total heat transfer area, $\dot{V}$ [m^{3}s^{-1}] – the volume flow rate, G [kgm^{-2}s^{-1}] – the mass velocity, and ΔT_{LMTD} – the logarithmic mean temperature difference and can be defined [16]:

$$\Delta T_{LMTD} = \frac{\left(T_w - T_{in}\right) - \left(T_w - T_{out}\right)}{\ln\left[\left(T_w - T_{in}\right) - \left(T_w - T_{out}\right)\right]} \tag{19}$$

Hydraulic diameter, D_h, and pressure drop, ΔP, can be calculated, respectively [23]:

$$D_h = \frac{2sh}{s+h} \tag{20}$$

$$\Delta P = P_{in} - P_{out} \tag{21}$$

The PEC used to evaluate thermal-hydraulic perfomance can be calculated [56]:

$$PEC = \frac{\dfrac{\mathrm{Nu}_{nf}}{\mathrm{Nu}_{bf}}}{\left(\dfrac{f_{nf}}{f_{bf}}\right)^3} \tag{22}$$

The subscripts nf and bf designate the base fluid and nanofluid, respectively.

Numerical procedures and mesh grid Independence analysis

In the present study, ANSYS FLUENT 2019 R3, one of the CFD dynamics software, is used for the numerical simulations. The SIMPLE algorithm is utilized to calculate the flow field, and the second order upwind scheme is used while discretizing the governing equations. Employing double precision solver, the solution is considered to have converged in case the residuals for each field are less than 10^{-6}. Mesh structure and the boundary-fitted grid are generated by using ICEM, one of the preprocessor in ANSYS, as illustrated in fig. 3. It is aimed to obtain the solutions precisely and accurately by increasing the grid densities near the walls. The mesh independence test is carried out for water (Re = 1000) in order to obtain the satisfactory solutions by employing different mesh patterns, as shown in fig. 4. Mesh independence analysis is conducted considering the *j* nad *f* results. It is seen that the change in *j* and *f* is not significant after the mesh number of $4.212 \cdot 10^6$, therefore, the optimum mesh number is determined as $4.212 \cdot 10^6$ for the computational domain in the present numerical analysis.

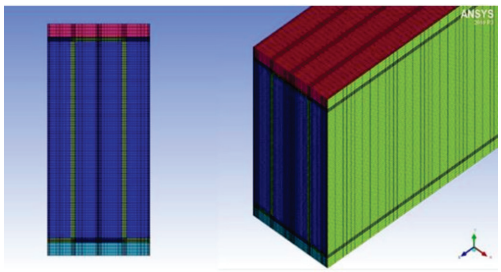

Figure 3. Mesh structure used in the present numerical study

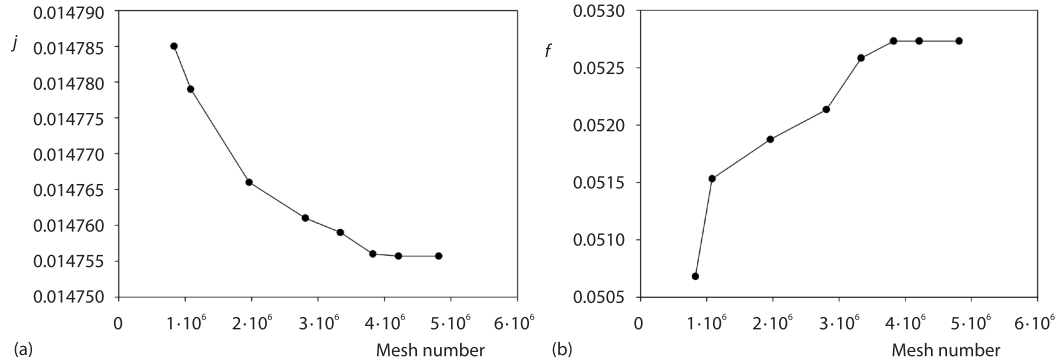

Figure 4. (a) Colburn *j*-factor and (b) Fanning friction factor *vs.* mesh number

Results and discussion

Model validation

Figure 5 shows the comparison of the values of the numerical j and f obtained from this study with the values obtained from the empirical correlations given by Wieting [7] using water as fluid. As can be seen in fig. 5, the numerical results obtained from the present study show similar trend with the results obtained from the empirical correlations given in literature. That is, j and f decrease with increasing Reynolds number as in [7]. It is seen that present numerical results are in good agreement with the literature results. The average error between the present numerical and empirical results are only 3.39% for j and 1.36% for f.

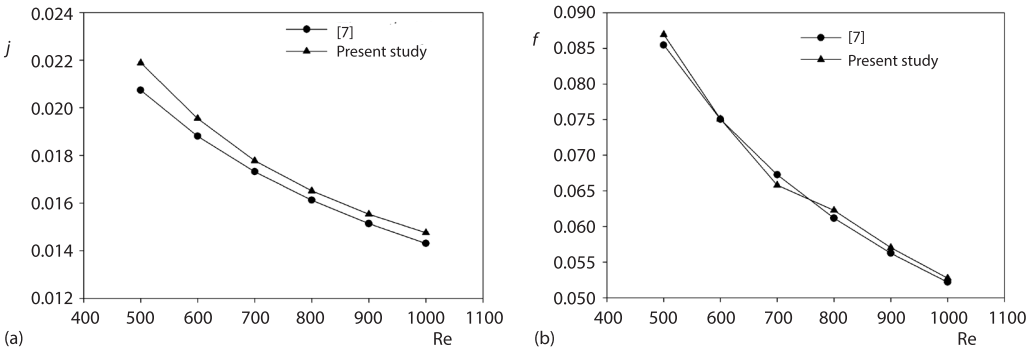

Figure 5. Validation study for water; (a) j and (b) f *vs.* Reynolds nimber

In addition, since there is no experimental study in the literature using nanofluid in the offset strip fins, the further validation was made according to a study [27] in which Al_2O_3-water nanofluid in the offset strip fins was analyzed numerically. The h and PP results are given as a function of Reynolds number in fig. 6. It is seen that there is a good agreement between the results of the present numerical study and the results of the study given in literature. Thus, it is reliable to solve the problem of flow and heat transfer in the created computational domain for offset strip fins.

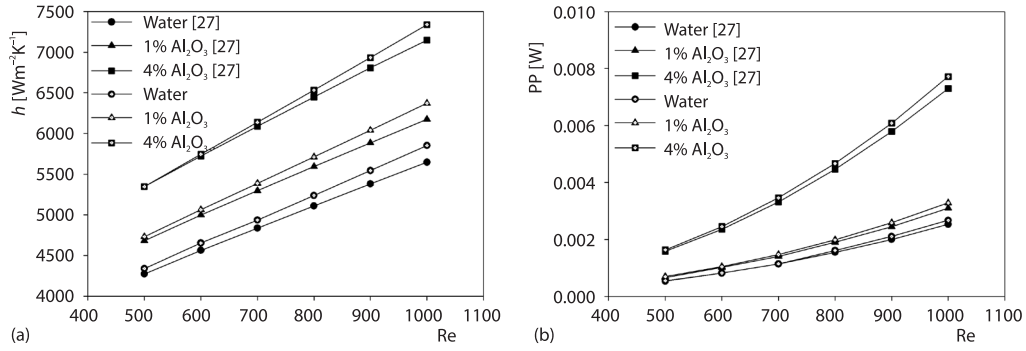

Figure 6. Validation study for Al_2O_3-water nanofluid; (a) h and (b) PP *vs.* Reynolds nimber

Heat transfer characteristics

The variations of $\dot{Q}$, h, and Nusselt number, are shown in figs. 7(a)-7(c), respectively, as a function of Reynolds number for TiO_2-water nanofluid. Figure 7(a) indicates the $\dot{Q}$ as a function of Reynolds number for TiO_2-water nanofluid at φ = 0-4% vol-

ume concentration range. It is seen that the heat transfer rate increases with increasing Reynolds number regardless of the volume concentration value. In addition, it is also seen that the volume concentration value is directly proportional to the heat transfer rate at any Reynolds number. As a result, it is obvious that heat transfer increases with the addition of TiO_2 nanoparticles into water. It is seen that, at Re = 1000, the heat transfer rate ratio $\dot{Q}_{nf}/\dot{Q}_{bf}$ are about 1.05, 1.10, 1.16, and 1.22 for 1%, 2%, 3%, and 4% volume concentrations of TiO_2 nanoparticle in base fluid, respectively. The reason for this increase in the heat transfer rate ratio may be that the nanofluid has higher inlet velocity and density than the base fluid. Therefore, its mass-flow rate is higher than that of water.

With regard to h, it is seen in fig. 7(b) that the average heat transfer coefficient increases with increasing both Reynolds number and nanoparticle volume concentration, φ, value. The maximum heat transfer coefficient ratio h_{nf}/h_{bf} is obtained as 1.31 at Re = 1000 and φ = 4%. The reason for this raise may be the effect of TiO_2 nanoparticles in the base fluid on the fin wall temperature.

Figure 7(c) shows the variation of Nusselt number as a function of Reynolds number at different φ. Similar to the situation in the heat transfer rate and heat transfer coefficient graphs, see figs. 7(a) and 7(b), the maximum value of Nusselt number is obtained at Re = 1000 and φ = 4%. Besides, the maximum Nusselt number ratio Nu_{nf}/Nu_{bf} is 1.19 at Re = 1000 and φ = 4%. In other words, dimensionless heat transfer coefficient Nusselt number increases 19% compared to base fluid water.

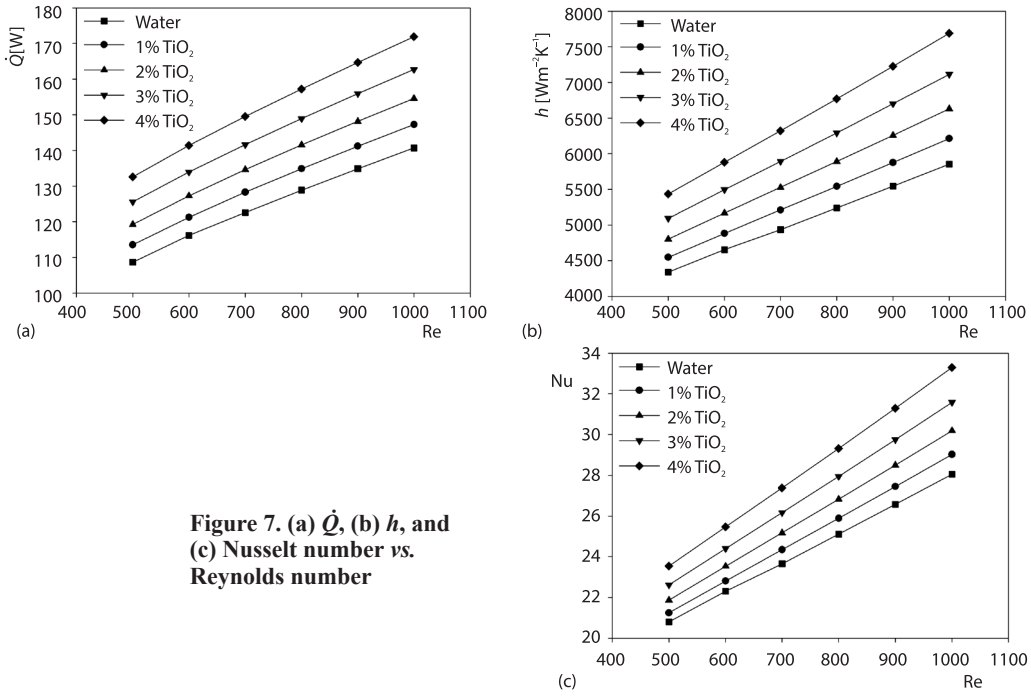

Figure 7. (a) $\dot{Q}$, (b) h, and (c) Nusselt number *vs.* Reynolds number

Pressure drop characteristics

The pressure drop, ΔP, and the associated PP are plotted in figs. 8(a) and 8(b), respectively, as a function of Reynolds number Re = 500-1000 at different volume concentrations φ = 0-4% of TiO_2-water nanofluid. It can be seen from fig. 8 that the pressure drop and the cor-

responding pumping power increase rapidly with increasing Reynolds number and nanoparticle volume concentration. To examine thoroughly the effect of the volume concentration of TiO_2 nanoparticle, *e.g.* at Re = 700, the values of the pressure drop ratio $\Delta P_{nf}/\Delta P_{bf}$ for 1%, 2%, 3%, and 4% nanofluids are 1.20, 1.42, 1.72, and 2.15, respectively. The reason for the increment in the pressure drop ratio may be that the viscosity and volume flow rate of TiO_2-water nanofluid are higher than that of water at the same Reynolds number. In addition, it is seen that, at the same Reynolds number, the values of pumping power ratio PP_{nf}/PP_{bf} for 1%, 2%, 3%, and 4% nanofluids are 1.27, 1.60, 2.10, and 2.89, respectively.

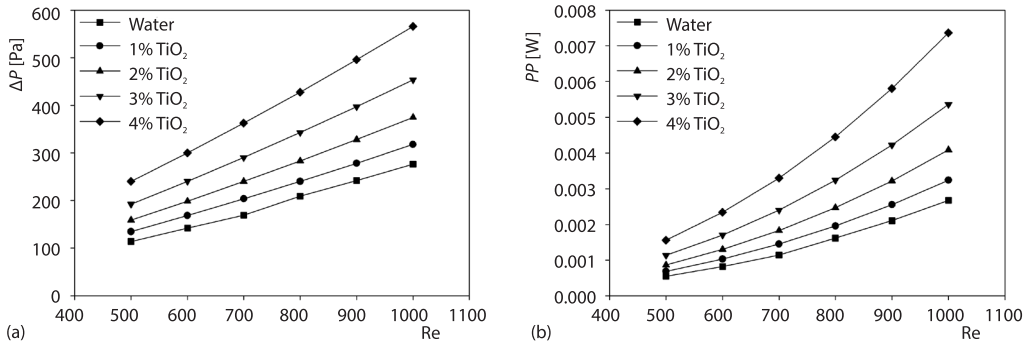

Figure 8. (a) Pressure drop and (b) pumping power *vs.* Reynolds number

Performance evaluation criteria

It is obvious that nanofluid added into base fluid increases heat transfer, fig. 7, in the rectangular offset strip fin modeled with increasing Reynolds number Re = 500-1000 for φ = 0-4% volume concentrations compared to water. However, it is seen that the *PP* to be used to compensate the ΔP also increases, fig. 8. In order to see whether the use of TiO_2-water nanofluid has an advantage for the rectangular offset strip fin, the dimensionless number called PEC is calculated using eq. (22). The PEC values are plotted in fig. 9 as a function of Reynolds number at different concentration values (φ = 0-4%) for TiO_2 nanoparticle. As seen in fig. 9, the PEC number is above unity for all concentration values in the range of φ =1-4% for the TiO_2 nanoparticle. For the comparison purposes, in fig. 9, the results for the Al_2O_3 nanoparticle is also given at φ =1 and 4%. As can be seen in fig. 9, the PEC number of TiO_2-water nanofluid is greater than that of Al_2O_3-water nanofluid. That is, the thermo-hydrodynamic performance of TiO_2-water nanofluid is greater than that of Al_2O_3-water nanofluid.

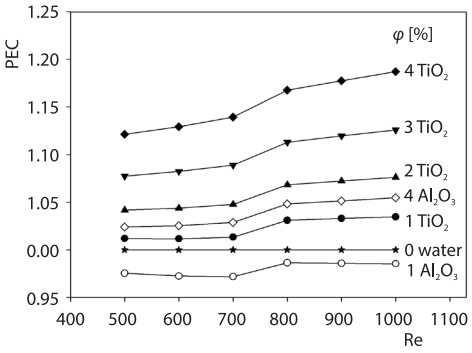

Figure 9. The PEC *vs.* Reynolds number at different φ

Conclusion

Single-phase laminar flow of TiO_2-water nanofluid in a rectangular offset strip fin is examined numerically. The thermal-hydraulic performance is investigated for φ = 0-4% volume concentration of the TiO_2 nanoparticle for the Reynolds number range Re = 500-1000. In addition, various numerical results are also obtained for Al_2O_3 nanoparticles for the validation

study. Results show that heat transfer rate and the required pumping power increase significantly with increasing volume concentration of the TiO_2 nanoparticles as compared to base fluid at the same Reynolds number. While heat transfer rate, heat transfer coefficient, and Nusselt number increase with increasing both Reynolds number and volume concentration of TiO_2 nanoparticles, both pressure drop, and pumping power also increase. It is seen that heat transfer rate, heat transfer coefficient, Nusselt number, pressure drop and pumping power reach their highest values when Re = 1000 and $\varphi = 4\%$. The PEC number for TiO_2 reaches its highest value in all Reynols numbers at $\varphi = 4\%$. The maximum PEC number value is 1.19 at Re = 1000 and $\varphi = 4\%$ for TiO_2-water nanofluid. It can be said that PEC number values are very promising at all volume concentration values examined in the laminar flow of TiO_2-water nanofluid. It can be said that TiO_2-water nanofluid is superior in terms of PEC values as compared to Al_2O_3-water nanofluid. This study may be useful for future researchers wishing to study nanofluid-flow in offset strip fin structure. It is hoped that the results obtained will contribute to the realization of the use of TiO_2-water nanofluid instead of conventional refrigerants in heavy vehicle radiators, where cooling performance is very important, and will guide future studies on this subject.

References

[1] Ismail, L. S., *et al.*, Numerical Study of Flow Patterns of Compact Plate-Fin Heat Exchangers and Generation of Design Data for Offset and Wavy Fins, *International Journal of Heat and Mass Transfer*, *52* (2009), 17-18, pp. 3972-3983
[2] Bergles, A.. Manglik, R., The Thermal-Hydraulic Design of the Rectangular Offset-Strip-Fin Compact Heat Exchanger, in: *Compact Heat Exchangers* (Eds. Shah, R. K., Kraus, A. D., and Metzger, D.), CRC press, New York, USA, 1990, pp. 123-149
[3] Bergles, A., *et al*., *Process, Enhanced, and Multi-phase Heat Transfer: A Festschrift for AE Bergles*, Begel House, New York, USA, 1996
[4] Manglik, R., Heat Transfer Enhancement, in: *Heat transfer handbook*, (Eds. Bejan, A., Kraus, A. D.), Wiley, Hoboken, N. J., USA, 2003, pp. 1029-1130
[5] Dong, J., *et al.*, Air-Side Thermal Hydraulic Performance of Offset Strip fin Aluminum Heat Exchangers, *Applied Thermal Engineering*, *27* (2007), 2-3, pp. 306-313
[6] Kenan, Y., Sahin, B., Flow-Induced Vibration Analysis of Conical Rings Used for Heat Transfer Enhancemen in Heat Exchanger, *Applied Energy, 78* (2004), 3, pp. 273-288
[7] Wieting, A. R., Empirical Correlations for Heat Transfer and Flow Friction Characteristics of Rectangular Offset-Fin Plate-Fin Heat Exchangers, *Journal of Heat Transfer*, *97* (1975), 3, pp. 488-490
[8] Sparrow, E. M., *et al*., Heat Transfer and Fluid-Flow Analysis of Interrupted-Wall Channels, with Application Heat Exchangers, *Journal of Heat Transfer*, *99* (1977), 1, pp. 4-11
[9] Shah, R. K., London, A. L., Offset Rectangular Plate-Fin Surfaces-Heat Transfer and Flow Friction Characteristics, *Journal of Engineering for Gas Turbines and Powe*r, *90* (1968), 3, pp. 218-228
[10] Joshi, H. M., Webb, R. L., Heat Transfer and Friction in the Offset Stripfin Heat Exchanger, *International Journal of Heat and Mass Transfer*, *30* (1987), 1, pp. 69-84
[11] Toossi, R., *et al*., Effect of Fluid Properties on Heat Transfer in Channels with Offset Strip fins, *Experimental Heat Transfer*, *7* (1994), 3, pp. 189-202
[12] Hu, S., Herold, K. E., Prandtl Number Effect on Offset Fin Heat Exchanger Performance: Experimental Results, *International Journal of Heat and Mass Transfe*r, *38* (1995), 6, pp. 1053-1061
[13] Michna, G. J., *et al*., An Experimental Study of the Friction Factor and Mass Transfer Performance of an Offset-Strip Fin array at Very High Reynolds Numbers, *Journal of Heat Transfer*, *129* (2007), 9, pp. 1134-1140
[14] Guo, L., *et al*., Lubricant Side Thermal-Hydraulic Characteristics of Steel Offset Strip Fins with Different Flow Angles, *Applied Thermal Engineering*, *28* (2008.), 8-9, pp. 907-914
[15] Fernandez-Seara, J., *et al*., Pressure Drop and Heat Transfer Characteristics of a Titanium Brazed Plate-Fin Heat Exchanger with Offset Strip Fins, *Applied Thermal Engineering*, *51* (2013), 1-2, pp. 502-511
[16] Khoshvaght-Aliabadi, M., *et al*., Experimental Analysis of Thermal-Hydraulic Performance of Copper-Water Nanofluid-Flow in Different Plate-Fin Channels, *Experimental Thermal and Fluid Science*, *52* (2014), Jan, pp. 248-258

[17] Jiang, Q., *et al.*, Thermal Hydraulic Characteristics of Cryogenic Offset-Strip Fin Heat Exchangers, *Applied Thermal Engineering*, *150* (2019), Mar., pp. 88-98
[18] De Losier, C. R., *et al*., The Parametric Study of an Innovative Offset Strip-Fin Heat Exchanger, *Journal of Heat Transfer*, *129* (2007), 10, pp.1453-1458
[19] Zhu, Y., Li, Y., The 3-D Numerical Simulation on the Laminar Flow and Heat Transfer in Four Basic Fins of Plate-Fin Heat Exchangers, *Journal of Heat Transfer*, *130* (2008), 11, 111801
[20] Bhowmik, H., Lee, K.-S., Analysis of Heat Transfer and Pressure Drop Characteristics in an Offset Strip Fin Heat Exchanger, *International Communications in Heat and Mass Transfer*, *36* (2009), 3, pp. 259-263
[21] Kim, M.-S., *et al.*, Correlations and Optimization of a Heat Exchanger with Offset-Strip Fins, *International Journal of Heat and Mass Transfer*, *54* (2011), 9-10, pp. 2073-2079
[22] Aliabadi, M. K., Hormozi, F., Performance Analysis of Plate-Fin Heat Exchangers: Different Fin Configurations and Coolants, *Journal of Thermophysics and Heat Transfer*, *27* (2013), 3, pp. 515-525
[23] Khoshvaght-Aliabadi, M., Hormozi, F., Effect of Wave-and-Lance Length Variations on Performance of Wavy and Offset Strip Plate-Fin Heat Exchangers, *Arabian Journal for Science and Engineering*, *38* (2013), 12, pp. 3515-3529
[24] Khoshvaght-Aliabadi, M., *et al*., Effects of Geometrical Parameters on Performance of Plate-Fin Heat Exchanger: Vortex-Generator as Core Surface and Nanofluid as Working Media, *Applied Thermal Engineering*, *70* (2014), 1, pp. 565-579
[25] Yang, Y., Li, Y., General Prediction of the Thermal Hydraulic Performance for Plate-Fin Heat Exchanger with Offset Strip Fins, *International Journal of Heat and Mass Transfer*, *78* (2014), Nov., pp. 860-870
[26] Yang, Y., *et al*., Analysis of the Fin Performance of Offset Strip Fins Used in Plate-Fin Heat Exchangers, *Journal of Heat Transfer*, *13*8 (2016), 10, 101801
[27] Zhao, N., *et al.*, Numerical Investigation of Laminar Thermal-Hydraulic Performance of Al_2O_3-water Nanofluids in Offset Strip Fins Channel, *International Communications in Heat and Mass Transfer*, *75* (2016), Apr., pp. 42-51
[28] Bhave, C. C., *et al.*, Computational Study of Enhanced Convection and Effects of Geometrical Features in Offset Strip Fin Cores, *Proceedings*, ASME 2017 Heat Transfer Summer Conference, Washington, D. C., USA, 2017
[29] Song, R., *et al.*, A Correlation for Heat Transfer and Flow Friction Characteristics of the Offset Strip Fin Heat exchanger, *International Journal of Heat and Mass Transfer*, *115* **(**2017), Dec., pp. 695-705
[30] Yang, Y., *et al.*, Heat Transfer Performances of Cryogenic Fluids in Offset Strip Fin-Channels Considering the Effect of Fin Efficiency, *International Journal of Heat and Mass Transfer*, *114* (2017), Nov., pp. 1114-1125
[31] Devireddy, S., *et al*., Improving the Cooling Performance of Automobile Radiator with Ethylene Glycol Water Based TiO_2 Nanofluids, *International Communications in Heat and Mass Transfer*, *78* (2016), Nov., pp. 121-126
[32] Leena, M., Srinivasan, S., Synthesis and Ultrasonic Investigations of Titanium Oxide Nanofluids, *Journal of Molecular Liquids*, *206* (2015), June., pp. 103-109
[33] Alam, T., Kim, M.-H., A Comprehensive Review on Single Phase Heat Transfer Enhancement Techniques in Heat Exchanger Applications, *Renewable and Sustainable Energy Reviews*, *81* (2018), 1, pp. 813-839
[34] Bigdeli, M. B., *et al*., A Review on the Heat and Mass Transfer Phenomena in Nanofluid Coolants with Special Focus on Automotive Applications, *Renewable and Sustainable Energy Reviews*, *60* (2016), July, pp. 1615-1633
[35] Gupta, M., *et al*., A Review on Thermophysical Properties of Nanofluids and Heat Transfer Applications, *Renewable and Sustainable Energy Reviews*, *74* (2017), July, pp. 638-670
[36] Gupta, M., *et al*., Up to Date Review on the Synthesis and Thermophysical Properties of Hybrid Nanofluids, *Journal of Cleaner Production*, *190* (2018), July, pp. 169-192
[37] Sidik, N. A. C., *et al*., Recent Advancement of Nanofluids in Engine Cooling System, *Renewable and Sustainable Energy Reviews*, *75* (2017), Aug., pp. 137-144
[38] Canbolat, A. S., *et al.*, Otomobil radyatörlerinde boru sayısının ısıl performansa ve etkenliğe etkisinin incelenmesi (in Turkish), *Proceedings*, 7th Automotive Technologies Congress, Bursa, Turkey, 2014
[39] Fard, M. H., *et al*., Numerical Study of Convective Heat Transfer of Nanofluids in a Circular Tube Two-Phase Model *vs*. Single-Phase Model, *International Communications in Heat and Mass Transfer*, *37* (2010), 1, pp. 91-97
[40] Lotfi, R., *et al.*, Numerical Study of Forced Convective Heat Transfer of Nanofluids: Comparison of Different Approaches, *International Communications in Heat and Mass Transfer*, *37* (2010), 1, pp. 74-78

[41] Akbari, M., *et al*., Comparative Assessment of Single and Two-Phase Models for Numerical Studies of Nanofluid Turbulent Forced Convection, *International Journal of Heat and Fluid-Flow*, *37* (2012), Oct., pp. 136-146
[42] Kalteh, M., *et al*., Experimental and Numerical Investigation of Nanofluid Forced Convection Inside a Wide Micro-Channel Heat Sink, *Applied Thermal Engineering*, *36* (2012), Apr., pp. 260-268
[43] Xuan, Y., Roetzel, W., Conceptions for Heat Transfer Correlation of Nanofluids, *International Journal of Heat and Mass Transfe*r, *43* (2000), 19, pp. 3701-3707
[44] Vajjha, R. S., *et al*., Numerical Study of Fluid Dynamic and Heat Transfer Performance of Al_2O_3 and CuO Nanofluids in the Flat Tubes of a Radiator, *International Journal of Heat and Fluid-Flow*, *31* (2010), 4, pp. 613-621
[45] Ganvir, R., *et al*., Heat Transfer Characteristics in Nanofluid – A Review, *Renewable and Sustainable Energy Reviews*, *75* (2017), Aug., pp. 451-460
[46] Khanafer, K., Vafai, K., A Critical Synthesis of Thermophysical Characteristics of Nanofluids, *International Journal of Heat and Mass Transfer*, *54* (2011), 19-20, pp. 4410-4428
[47] Vajjha, R. S., Das, D. K., Experimental Determination of Thermal Conductivity of Three Nanofluids and Development of New Correlations, *International Journal of Heat and Mass Transfer*, *52*(2009), 21-22, pp. 4675-4682
[48] Maxwell, J. C., *A Treatise on Electricity and Magnetism*, Clarendon Press, Oxford, UK, 1881
[49] Duangthongsuk, W., Wongwises, S., Measurement of Temperature-Dependent Thermal Conductivity and Viscosity of TiO_2-Water Nanofluids, *Experimental Thermal and Fluid Science*, *33* (2009), 4, pp. 706-714
[50] Corcione, M., Heat Transfer Features of Buoyancy-Driven Nanofluids Inside Rectangular Enclosures Differentially Heated at the Sidewalls, *International Journal of Thermal Sciences*, *49* (2010), 9, pp. 1536-1546
[51] Xie, H., *et al*., The MgO Nanofluids: Higher Thermal Conductivity and Lower Viscosity among Ethylene Glycol-Based Nanofluids Containing Oxide Nanoparticles, *Journal of Experimental Nanoscienc*e, *5* (2010), 5, pp. 463-472
[52] Azmi, W., *et a*l., Nanofluid Properties for Forced Convection Heat Transfer: An Overview, *Journal of Mechanical Engineering and Sciences*, *4* (2013), June, pp. 397-408
[53] Milanese, M., *et al*., High Efficiency Nanofluid Cooling System for Wind Turbines, *Thermal Science*, *18* (2014), 2, pp. 543-554
[54] Akyurek, E. F., *et al*., The Experimental Investigation of the Viscosity of the Al_2O_3 Nanofluid, *Eastern Anatolian Journal of Science*, *V* (2019), II, pp. 26-35
[55] Khoshvaght-Aliabadi, M., *et al*., Role of Channel Shape on Performance of Plate-Fin Heat Exchangers: Experimental Assessment, *International Journal of Thermal Sciences*, *79* (2014), May, pp. 183-193
[56] Webb, R., Performance Evaluation Criteria for Use of Enhanced Heat Transfer Surfaces in Heat Exchanger Design, *International Journal of Heat and Mass Transfer*, *24* (1981), 4, pp. 715-726

Paper submitted: October 19, 2020
Paper revised: December 8, 2020
Paper accepted: December 21, 2020